Probing structural differences between PrPC and PrPSc by surface nitration and acetylation: Evidence of conformational change in the C-terminus

7 AUTHORS, INCLUDING:

Adriana Ramos
Johns Hopkins Medicine
12 PUBLICATIONS **98** CITATIONS

SEE PROFILE

Ester Vazquez Fernandez
University of Alberta
4 PUBLICATIONS **63** CITATIONS

SEE PROFILE

Jana Alonso
University of Oxford
33 PUBLICATIONS **295** CITATIONS

SEE PROFILE

Zengshan Liu
Jilin University
38 PUBLICATIONS **230** CITATIONS

SEE PROFILE

Probing structural differences between PrP^C and PrP^{Sc} by surface nitration and acetylation: evidence of conformational change in the C-terminus

Binbin Gong,[†,‡] Adriana Ramos,[‡] Ester Vázquez-Fernández,[‡] Christopher J. Silva,[§] Jana Alonso,[∥] Zengshan Liu,[†] and Jesús R. Requena*[,‡]

[†]Key Laboratory of Zoonosis Research, Ministry of Education, Institute of Zoonosis, College of Animal Science and Veterinary Medicine, Jilin University, Changchun, P. R. China

[‡]Department of Medicine, University of Santiago de Compostela, Santiago de Compostela, Galiza, Spain

[§]Western Regional Research Center, United States Department of Agriculture, Albany, California 94710, United States

[∥]Laboratory of Proteomics, IDIS, Santiago de Compostela, Spain

S *Supporting Information*

ABSTRACT: We used two chemical modifiers, tetranitromethane (TNM) and acetic anhydride (Ac$_2$O), which specifically target accessible tyrosine and lysine residues, respectively, to modify recombinant Syrian hamster PrP(90−231) [rSHaPrP(90−231)] and SHaPrP 27−30, the proteinase K-resistant core of PrP^{Sc} isolated from brain of scrapie-infected Syrian hamsters. Our aim was to find locations of conformational change. Modified proteins were subjected to in-gel proteolytic digestion with trypsin or chymotrypsin and subsequent analysis by mass spectrometry (MALDI-TOF). Several differences in chemical reactivity were observed. With TNM, the most conspicuous reactivity difference seen involves peptide E$_{221}$−R$_{229}$ (containing Y$_{225}$ and Y$_{226}$), which in rSHaPrP-(90−231) was much more extensively modified than in SHaPrP 27−30; peptide H$_{111}$−R$_{136}$, containing Y$_{128}$, was also more modified in rSHaPrP(90−231). Conversely, peptides Y$_{149}$−R$_{151}$, Y$_{157}$−R$_{164}$, and R$_{151}$−Y$_{162}$ suffered more extensive modification in SHaPrP 27−30. Acetic anhydride modified very extensively peptide G$_{90}$−K$_{106}$, containing K$_{101}$, K$_{104}$, K$_{106}$, and the amino terminus, in both rSHaPrP(90−231) and SHaPrP 27−30. These results suggest that (1) SHaPrP 27−30 exhibits important conformational differences in the C-terminal region with respect to rSHaPrP(90−231), resulting in the loss of solvent accessibility of Y$_{225}$ and Y$_{226}$, very solvent-exposed in the latter conformation; because other results suggest preservation of the two C-terminal helices, this might mean that these are tightly packed in SHaPrP 27−30. (2) On the other hand, tyrosines contained in the stretch spanning approximately Y$_{149}$−R$_{164}$ are more accessible in SHaPrP 27−30, suggesting rearrangements in α-helix H1 and the short β-sheet of rSHaPrP(90−231). (3) The amino-terminal region of SHaPrP 27−30 is very accessible. These data should help in the validation and construction of structural models of PrP^{Sc}.
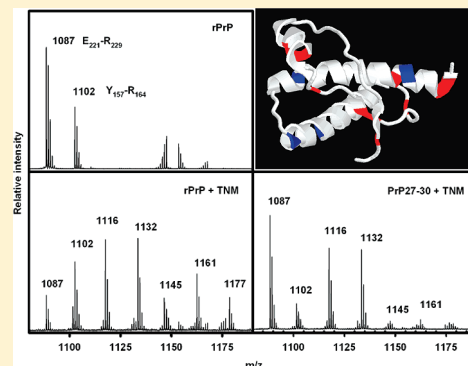
P rions are infectious proteins. They facilitate the conversion of a native nonprionic conformational isoform of themselves into the prion conformation through a molecular mechanism that is not fully understood but likely involves templating and/or stabilization by means of ordered aggregation.[1−3] As more and more units of the native protein in the non-prion conformation are refolded into the prion conformation, the conversion process accelerates. Some prions, like Sup32 and Ure2p, found in yeasts, lack the functional properties of their progenitor proteins, lost as a consequence of the conformational transition.[4] Others, like Het-s, found in the fungus *Podospora anserina*, exhibit an alternative functionality as compared to that of the progenitor protein.[4] CPEB, a protein from the sea hare *Aplysia* that has been proposed to have a role in long-term memory, has characteristics that suggest it has prion-like properties.[5] In stark contrast with these innocuous or even functional prions, the

mammalian prion, PrP^{Sc}, the first prion to be identified, causes and transmits fatal neurodegenerative diseases, termed transmissible spongiform encephalopathies, that affect humans and valuable farm animals.[1,2,6−8] In humans, PrP^{Sc} arises sporadically as a very rare event with an approximate incidence of 1 in 1 million cases/year, causing sporadic forms of Creutzfeldt-Jakob disease and fatal familial insomnia. PrP^{Sc} also arises as a consequence of mutations in the *PRNP* gene that supposedly result in the instability of PrP^C, its normal conformational precursor. Once PrP^{Sc} appears, it spreads throughout the affected brain, converting available PrP^C into PrP^{Sc}. In parallel with the accumulation of PrP^{Sc}, pathological changes develop in the brain,

including death of neurons and gliosis, in a course that invariably leads to death.[1,2,6] Transmission between individuals can occur as a consequence of iatrogenic procedures, such as reutilization of PrP^{Sc}-contaminated surgical instruments[6,7] or blood transfusion.[7] Oral transmission can also take place through consumption of PrP^{Sc}-containing animal tissues. This occurred during the bovine spongiform encephalopathy (BSE) epidemic when prion-infected tissue from domestic cattle was rendered and then fed to a variety of animals. During the BSE epidemic, a zoonotic disease, variant CJD, emerged from the consumption of prion-contaminated animal tissue by humans.[1,7,8]

How prions propagate is not fully understood. All known prions are amyloids. A nucleated polymerization model has been invoked to explain some aspects of the conversion process. According to this model, individual molecules with the prion conformation would assemble to form an oligomer. Once it reaches a critical size, it would become stable and would further nucleate stable growth.[9] This is basically the mechanism by which amyloids grow in vitro, and therefore, prions would just be amyloids with particular properties of resilience that allow them to be transmitted between organisms. In any case, knowledge of their structure is essential to understanding the mechanism of their propagation. In the particular case of PrP^{Sc}, such knowledge should also help in our understanding of some critical features of transmission, namely, the existence of strains and transmission barriers. Strains are subtypes of a given PrP^{Sc} that exhibit distinct biochemical and biophysical properties and cause distinct disease phenotypes, all of which is maintained in a stable way throughout transmission.[1,10] It is believed that strain characteristics are enciphered by subtle conformational differences in PrP^{Sc} structure.[11,12] Transmission barriers between species are thought to be the result of the limited ability of the native PrP^{C} of one species to adopt the conformation enciphered by the PrP^{Sc} of another species. For example, BSE prions transmit very easily to cattle but very inefficiently to humans or mice expressing human PrP. In contrast, the barrier for transmission of ovine scrapie prions to humans is so high that no cases of transmission have been documented thus far. Transmission barriers are also believed to be caused by relations of structural compatibility between the incoming PrP^{Sc} molecules and the host PrP molecules.[1,2]

Unfortunately, the insoluble nature of PrP^{Sc} has hampered efforts to determine its structure, preventing the use of high-resolution techniques such as NMR or X-ray crystallography. Therefore, only partial structural information has been painstakingly gathered from low-resolution approaches such as FTIR,[13−15] electron microscopy,[16−20] limited proteolysis,[11,21−23] chemical cross-linking with bifunctional reagents,[24] immunoassays,[25,26] and fiber X-ray diffraction.[27,28]

Surface labeling using chemical reagents is another low-resolution technique that can be used to probe the structure of macromolecules. In fact, nitration of tyrosine residues has been used to study structural differences between recombinant mono-meric PrP, folded in the PrP^{C} conformation, and a β sheet-rich oligomer obtained by incubation of unfolded recombinant PrP in pH 3.7 buffer containing 3.6 M urea.[29] Here, we describe studies aimed at probing structural differences between rSHaPrP and PrP^{Sc} isolated from brains of scrapie-infected hamsters.

■ EXPERIMENTAL PROCEDURES

Reagents and Proteins. Trypsin (sequencing grade, modified) was obtained from Promega (Madison, WI); chymotrypsin and

N-glycosidase F (PNGase F) were from New England Biolabs (Beverly, MA). All other reagents were from Sigma-Aldrich. We prepared rSHaPrP(90−231) as previously described[30] and stored it as a 1 mg/mL solution in 6 M guanidine hydrochloride. It was refolded by 1:10 dilution in PBS for 30 min at room temperature (RT) and then concentrated as desired by ultra-filtration (Amicon Ultra, 10K, Millipore, Carrigtwahill, Ireland). rSHaPrP(90−231) refolded by this procedure is known to closely resemble SHaPrP^{C},[30] and CD spectroscopy analysis shows that it displays the characteristic absorption minima of a predominantly α-helical protein.[31] SHaPrP 27−30 was isolated as described previously from brains of terminally ill Syrian hamsters infected with the 263K strain of scrapie.[32] Briefly, 10% brain homogenates prepared in 10% sarkosyl-containing buffer were clarified by centrifugation, and the supernatant, containing most PrP^{Sc}, was subjected to several cycles of high-force centrifugation and extraction in aqueous buffers containing different amounts of detergent. Treatment with proteinase K (PK) converted full-length PrP^{Sc} into its PK-resistant amino-terminally truncated derivative PrP 27−30. The final product was suspended in 1% sarkosyl, and its purity was assessed by SDS−PAGE. Its concentration was measured with the BCA Protein Assay Kit (Pierce, Rockford, IL) as described previously.[33]

Chemical Modifications. For chemical modification of lysine residues, rSHaPrP(90−231) and SHaPrP 27−30 were mixed with a 3000-fold molar excess of Ac$_2$O to protein (333-fold excess over reactive amino groups, including eight lysine residues and the amino terminus) in 40 μL of 100 mM phosphate buffer (pH 7.4), at a protein concentration of 0.6 μg/mL. Reactions were allowed to proceed for 15 min at RT and then stopped by addition of 10% trifluoroacetic acid (TFA) to a final concentra-tion of 1%. For chemical modification of tyrosine residues, a stock solution of 6 mg/mL TNM was prepared in 95% ethanol. rSHaPrP(90−231) and SHaPrP 27−30 were mixed with a 200-fold molar excess of TNM to protein (20-fold molar excess over tyrosine residues) in 40 μL of 100 mM phosphate (pH 7.4), at a final concentration of 0.6 μg/mL. Reactions were allowed to proceed for 1 h at RT and then stopped by addition of β-mercaptoethanol at a final concentration of 5% (w/v).

Deglycosylation and Electrophoretic Separation. After reaction with Ac$_2$O, modified and control SHaPrP 27−30 were precipitated via addition of ice-cold methanol to a final concen-tration of 85% and kept at 4 °C for 30 min. Samples were spun at 20000g for 20 min in a tabletop centrifuge. Pellets were then denatured and deglycosylated with 3 μL of a PNGase F solution at 37 °C for 48 h, according to the manufacturer's instructions. Reaction mixtures were then precipitated in 200 μL of 85% methanol. After reaction with TNM, modified and control SHaPrP 27−30 were precipitated with 85% methanol as de-scribed. All the pellets were resuspended in 20 μL of reducing Laemmli sample buffer, boiled for 10 min, and subjected to SDS−PAGE[34] using 12% gels. Protein bands were stained with Coomassie blue.

In-Gel Proteolytic Digestion. For samples analyzed by MAL-DI-TOF, protein bands were carefully excised with a razor blade and then reduced, alkylated, and digested in-gel with trypsin or chymotrypsin, according to the procedure of Shevchenko et al.[35] with slight modifications. Briefly, bands were cut into 1 mm^3 pieces, placed in an Eppendorf tube, washed with water, and dehydrated with 200 μL of acetonitrile for 15 min using mild agitation. Acetonitrile was removed, and the gel pieces were dried in vacuo (SpeedVac, Savant, Farmingdale, CA); a volume of 30

μL of 10 mM DTT in 25 mM NH$_4$HCO$_3$ was added, and reduction was conducted at 37 °C for 60 min. The solvent was then removed and, after dehydration of gel pieces with acetonitrile as described, replaced with 30 μL of 55 mM iodoacetamide. Alkylation was conducted in the dark at RT for 20 min. The solvent was then removed, and gel pieces were washed with 25 mM NH$_4$HCO$_3$, dehydrated with acetonitrile, and rehydrated on ice via addition of 20 μL of 25 mM NH$_4$HCO$_3$ containing 10 ng/μL trypsin or chymotrypsin. After 40 min, 30 μL of 25 mM NH$_4$HCO$_3$ was added to cover the gel pieces, and samples were incubated overnight at 37 °C. Digested samples were briefly centrifuged, and the supernatant was collected. Gel pieces were then extracted with 20 μL of 25 mM NH$_4$HCO$_3$ with sonication for 10 min. The solvent was then recovered and replaced with 20 μL of 0.1% TFA. The extracts and the digestion solution were pooled and dried in vacuo for further MALDI-TOF analysis.

MALDI-TOF. Dried samples were dissolved in 10 μL of 20% acetonitrile in 0.5% HCOOH. Equal volumes (0.5 μL) of peptide and matrix solution, consisting of 3 mg of (R)-cyano-4-hydroxy-cinnamic acid (α-CHC) dissolved in 1 mL of 50% acetonitrile in 0.1% TFA, were deposited using the thin layer method onto a 384 Opti-TOF MALDI plate (Applied Biosystems). MALDI analyses were performed in a model 4800 MALDI-TOF/TOF analyzer (Applied Biosystems). MS spectra were acquired in reflectron positive-ion mode with a Nd:YAG, 355 nm wavelength laser, averaging 1000 laser shots. Resulting peaks were internally calibrated using at least three trypsin autolysis peaks in the case of tryptic peptides and externally calibrated using a peptide mix standard (bradykinin 1−7, angiotensin II, angiotensin I, substance P, bombesin, rennin substrate, ACTH clip 1−17, ACTH clip 18−39, and somatostatin 28 from Bruker Daltonics) for peptides produced by chymotrypsin digestion. Mass assignment and peptide identification were conducted using GPMAW 6.01 (Lighthouse, Odense, Denmark). MS/MS analyses were performed by selection of the precursor with an absolute mass window of ±0.5 Da and metastable suppressor. In the MS/MS 1 kV analysis mode, the precursor was accelerated to 8 kV in source 1, and fragment ions were further accelerated by 15 kV in source 2.

Immunodetection of Chemically Modified Epitopes. Brain homogenates (10%) of scrapie-infected and control Syrian hamsters were prepared in PBS containing 1% sarkosyl. Samples were treated with TNM or Ac$_2$O (vide supra); the ratio of these agents to total protein in the homogenates was the same as the ratio of the agents to PrP in the experiments described above. All reaction mixtures were then precipitated in 85% methanol. Pellets were resuspended with 20 μL of reducing Laemmli sample buffer, boiled for 10 min, and subjected to SDS−PAGE as described above. Gels were transferred to nitrocellulose membranes and probed with antibody R1 (InPro, San Francisco, CA) that recognizes an epitope within the C-terminal segment of amino acid residues, Y$_{225}$YDGRRS$_{231}$,[25] or with antibody 3F4 (Signet, Emeryville, CA) that recognizes epitope M$_{109}$KHM$_{112}$, each at a 1:5000 dilution. Peroxidase-labeled anti-human or anti-mouse antibodies were used as the secondary antibody, both at a 1:5000 dilution. Blots were developed with ECL-plus reagent (GE Healthcare, Little Chalfont, U.K.).

RESULTS

Nitration Reaction. The ratio of TNM to PrP protein was chosen so that it was in agreement with previous studies to avoid an excessive modification of PrP that might induce conformational
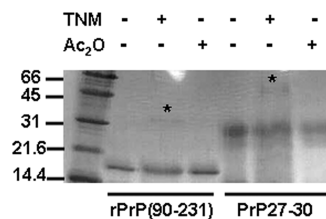

Figure 1. SDS−PAGE analysis of the reaction of TNM and Ac$_2$O with SHaPrP 27−30 and rSHaPrP(90−231). Asterisks signal faint bands corresponding to dimers in samples treated with TNM. SHaPrP 27−30 samples were not deglycosylated with PNGase F in this experiment; therefore, the mass of PrP appears to be higher as a consequence of the attached carbohydrates. The gel was stained with Coomassie blue.

changes during the reaction.[29,36] Consequently, SDS−PAGE analysis of chemically modified samples showed that the majority of protein molecules remained monomeric (Figure 1), similar to what was observed by Lennon et al. in their study of nitration of the α-rich and β-rich isoforms of recombinant PrP.[29] Tryptic digestion of rSHaPrP(90−231) generates six tyrosine-containing peptides: H$_{111}$-(Y$_{128}$)-R$_{136}$, Y$_{149}$-(Y$_{150}$)-R$_{151}$, Y$_{157}$-(Y$_{162}$,Y$_{163}$)-R$_{164}$, P$_{165}$-(Y$_{169}$)-K$_{185}$, V$_{209}$-(Y$_{218}$)-K$_{220}$, and E$_{221}$-(Y$_{225}$,Y$_{226}$)-R$_{229}$. All of these peptides, except P$_{165}$-(Y$_{169}$)-K$_{185}$, were detected by MALDI (Figure 2). P$_{165}$-(Y$_{169}$)-K$_{185}$, with a monoisotopic molecular mass of 2474.15 Da, is the largest among them, and failure to detect it probably reflects poor recovery after in-gel digestion. Treatment of rSHaPrP(90−231) and SHaPrP 27−30 resulted in evident decreases in the relative intensities of the signals of some peptides (Figure 2) with the concomitant appearance of new peaks corresponding to peptides containing nitrated tyrosine residues. Nitration of one tyrosine residue results in a mass increase of 45 Da (substitution of H with NO$_2$); however, subsequent laser-induced loss of one or two oxygen atoms, during MALDI, yields species with mass increases of 29 and 13 Da.[29] Nitration of more than one tyrosine results in peptides exhibiting mass increases that correspond to combinations of these numbers, i.e., 26, 42, 58, 74, and 90. Examples of these nitrated peptides can be seen in Figures 3 and 4, which show expanded views of the MALDI-TOF spectra in the m/z regions near the peaks corresponding to E$_{221}$-(Y$_{225}$,Y$_{226}$)-R$_{229}$ and Y$_{149}$-(Y$_{150}$)-R$_{151}$, respectively. Of the five tyrosine-containing peptides detected, four were nitrated as a result of the reaction of TNM with rSHaPrP(90−231). The extent of nitration of each peptide was calculated as the ratio of the sum of areas of peaks corresponding to nitrated peptides over the sum of all areas corresponding to the precursor peptide and its nitrated derivatives; results are shown in a semiquantitative way in Table 1. The most extensively nitrated peptide was E$_{221}$-(Y$_{225}$,Y$_{226}$)-R$_{229}$ (Table 1). The presence of species with m/z increases of 26, 58, 90, etc., indicates that both Y$_{225}$ and Y$_{226}$ react with TNM, in excellent agreement with the extreme solvent exposure of these two residues in rSHaPrP (Protein Data Bank entry 1B10). Peptide H$_{111}$-(Y$_{128}$)-R$_{136}$ exhibited a moderate level of nitration (Table 1); because there is only one tyrosine residue in this peptide, Y$_{128}$, it can be concluded that this residue is only moderately nitrated by TNM, in agreement with its partial solvent exposure. Peptides Y$_{149}$-(Y$_{150}$)-R$_{151}$ and Y$_{157}$-(Y$_{162}$, Y$_{163}$)-R$_{164}$ exhibited very modest nitration, and peptide V$_{209}$-(Y$_{218}$)-K$_{220}$ exhibited no nitration at all (Table 1). Y$_{150}$ is completely buried within PrP^C. Y$_{157}$, Y$_{163}$, and Y$_{218}$ are partially buried, while Y$_{149}$ and Y$_{162}$ are relatively solvent accessible.
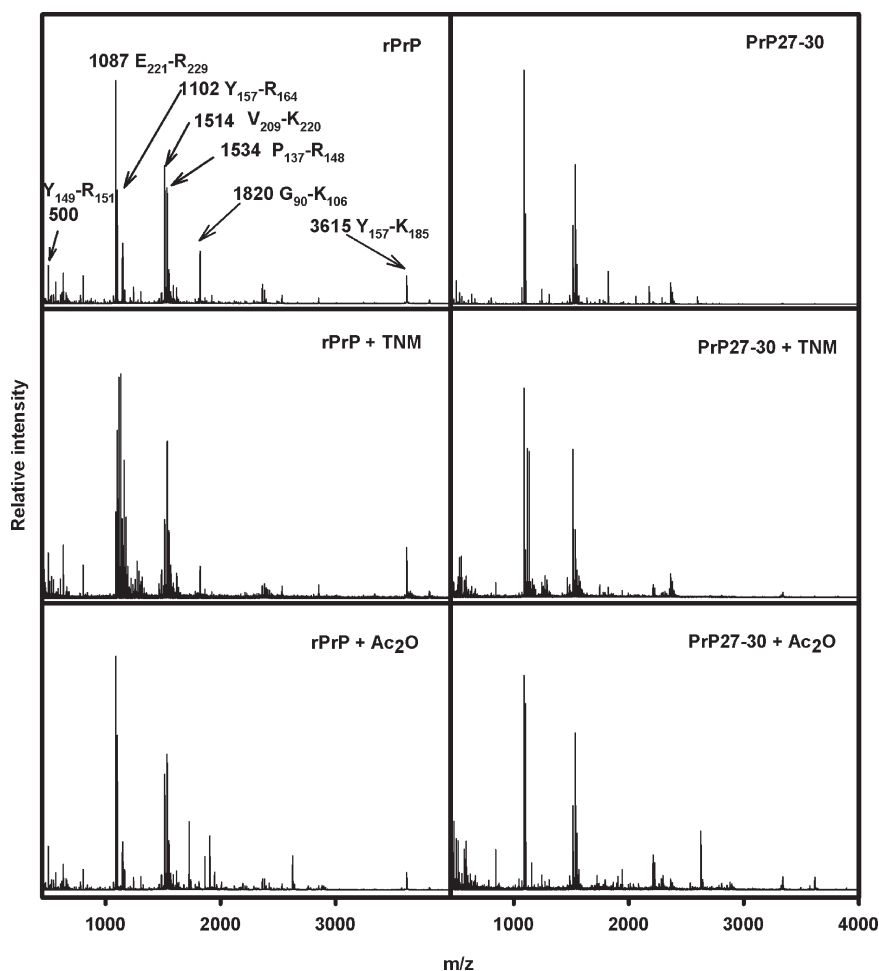
Figure 2. MALDI-TOF spectrum of the tryptic digest of SHaPrP 27−30 and rSHaPrP(90−231), and rSHaPrP 27−30 and rSHaPrP(90−231) treated with TNM or Ac₂O. For a complete list of identified peaks, see the text (Results).

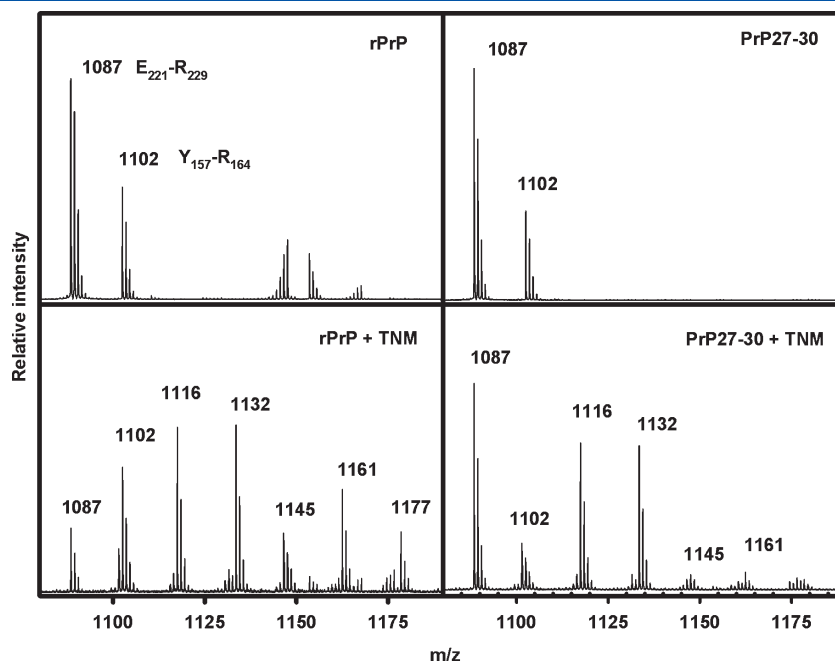**Figure 3.** Close-up of the m/z 1100 region of the spectrum shown in Figure 2, corresponding to control and TNM-treated samples. Peaks with m/z values of +45, +29, and +13 reflect nitration, deoxy nitration, and dideoxy nitration, respectively.
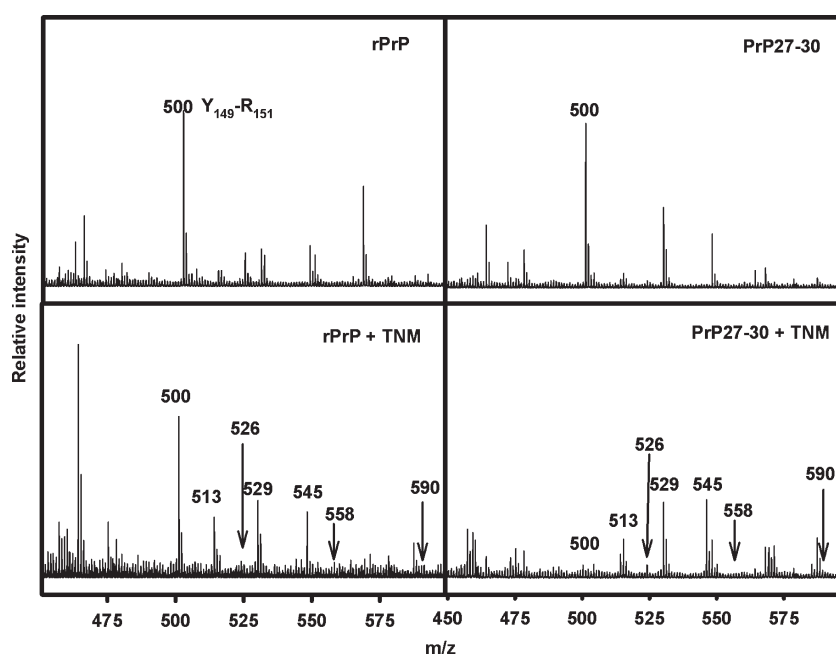
Figure 4. Close-up of the m/z 500 region of the spectrum shown in Figure 2, corresponding to control and TNM-treated samples. Peaks with m/z values of +45, +29, and +13 (545, 529, and 513) reflect nitration, deoxy nitration, and dideoxy nitration, respectively. Arrows indicate places where peaks corresponding to dinitration of $Y_{149}-R_{151}$, not detected, should have been seen.

Table 1. MALDI-TOF Analysis of rSHaPrP(90−231) and SHaPrP 27−30 Peptides Produced by Trypsin Digestion after TNM or Ac$_2$O Modification^a

experimental mass (Da)	theoretical mass (Da)	peptide and sequence	rSHaPrP	PrP 27−30
		TNM Reaction		
2362.13	2362.13	(111)HMAGAAAAG...GYMLGSAMSR(136)	++	+
500.24	500.24	(149)YYR(151)	++	++++
1101.52	1101.50	(157)YPNQVYYR(164)	++	+++
1513.69	1513.69	(209)VVEQMCTTQYQK(220)	−	−
1087.46	1087.46	(221)ESQAYYDGR(229)	++++	++
		Ac$_2$O Reaction		
1819.99	1819.90	(90)GQGGGTHNQWNKPSKPK(106)	++++	++++

^{a} Nitration or acetylation was calculated as (sum of the areas of modified peaks)/(sum of the areas of all peaks) and expressed as 0−10% (−), 11−30% (+), 31−60% (++), 61−80% (+++) and 81−100% (++++). Data represent means of three independent experiments.

The pattern of nitration of SHaPrP 27−30 was strikingly different. Peptides E_{221}-(Y_{225},Y_{226})-R_{229} and H_{111}-(Y_{128})-R_{136} showed a very significantly reduced level of nitration as compared with that of rSHaPrP(90−231), while in contrast, peptides Y_{149}-(Y_{150})-R_{151} and Y_{157}-(Y_{162},Y_{163})-R_{164} had the opposite behavior and showed increased levels of nitration. We found no evidence of the presence of dinitrated species of Y_{149}-(Y_{150})-R_{151} (Figure 4), indicating that only one of the two tyrosine residues contained in this peptide is significantly nitrated. We subjected to MS/MS analysis the ion $[MH]^+$ at m/z 530, which corresponds to mononitrated Y_{149}-(Y_{150})-R_{151} (m/z +29 species); the MS/MS spectrum shows the presence of ions y_2 + 29 and b_2 + 29 but just traces of y_2 and b_2 (Figure 1 of the Supporting Information), which identifies Y_{150} as the predominantly nitrated residue. Similar results were obtained with the ion $[MH]^+$ at m/z 546 (data not shown). In contrast to this peptide, peaks corresponding to mono- and dinitrated Y_{157}-(Y_{162},Y_{163})-R_{164} were detected. This means that at least Y_{162} or Y_{163} becomes increasingly nitrated in SHaPrP 27−30, as compared to rSHaPrP(90−231), suggesting a structural change that specifically affects the second short β-strand in PrP^C. We tried to identify whether Y_{162}, Y_{163}, or both are preferential targets of nitration in SHaPrP 27−30 by means of MS/MS experiments, but our efforts failed as a consequence of the impossibility of isolating the relevant precursor ions from ions corresponding to variably nitrated E_{221}-(Y_{225},Y_{226})-R_{229} exhibiting partially overlapping isotopic distributions.

Peptide H_{111}-(Y_{128})-R_{136}, and therefore Y_{128}, also exhibited significantly less nitration in SHaPrP 27−30 with respect to rSHaPrP(90−231).

We performed additional in-gel digestion of nitrated and control samples using chymotrypsin (Table 2). Results agree very well with those obtained with trypsin digestion. Thus, peptide R_{151}-(Y_{157})-Y_{162} and the same peptide with an oxidized methionine, a result of sample manipulation, were only modestly nitrated in rSHaPrP(90−231) but significantly more so in

Table 2. MALDI-TOF Analysis of rSHaPrP(90−231) and SHaPrP 27−30 Peptides Produced by Chymotrypsin Digestion after TNM Modification[a]

experimental mass (Da)	theoretical mass (Da)	peptide and sequence	rSHaPrP	PrP 27−30
1053.42	1053.59	(142)GNDWEDRY(149)	[c]	[c]
1216.48	1216.58	(142)GNDWEDRYY(150)	−	++
776.38	776.41	(164)RPVDQY(169)	++	++
1582.73	1582.85	(151)RENMNRYPNQVY(162)	++	+++
1598.73	1598.85	(151)RENM(O)NRYPNQVY(162)[b]	++	+++

[a] Nitration was calculated as (sum of the areas of modified peaks)/(sum of the areas of all peaks) and expressed as 0−10% (−), 31−60% (++), and 61−80% (+++). [b] In this peptide, methionine was oxidized as a consequence of sample manipulation; correspondingly, a peak at m/z +16 was produced. [c] The extent of nitration could not be assessed as a consequence of the presence of interfering peaks of overlapping masses.
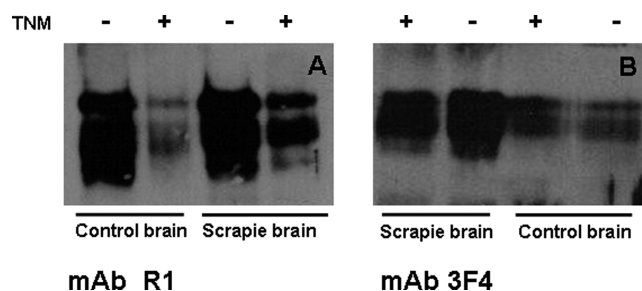

Figure 5. Epitope masking analysis of scrapie-infected and control brain homogenates. Samples were treated with TNM or buffer alone and subjected to WB analysis. (A) Samples probed with antibody R1 that recognizes epitope $Y_{225}YDGRRS_{231}$. (B) Samples probed with antibody 3F4 that recognizes epitope $M_{109}KHM_{112}$.

SHaPrP 27−30. This agrees with data obtained for peptide Y_{157}-(Y_{162},Y_{163})-R_{164}. Likewise, peptide G_{142}-(Y_{149})-Y_{150} was also significantly more nitrated in SHaPrP 27−30 than in rSHaPrP(90−231), in agreement with results for the tryptic peptide Y_{149}-(Y_{150})-R_{151}.

Because the GPI anchor in SHaPrP 27−30 might exert steric hindrance, decreasing the availability of Y_{225} and Y_{226} for reaction with TNM and comparing SHaPrP 27−30 to rSHaPrP(90−231) being inappropriate, we sought to assess the reactivity of these tyrosine residues in GPI-containing PrP^C present in brain homogenate. For this, we took advantage of the fact that these residues lie within the epitope recognized by antibody R1.[25] Therefore, reaction of these residues with TNM should weaken binding of R1. As expected, WB analysis showed a more marked decrease in the intensity of TNM-treated versus untreated control samples as compared with scrapie-infected samples (Figure 5A), in agreement with a more extensive nitration of the epitope in PrP^C. In contrast, no decreases in intensity were seen in blots probed, after nitration, with antibody 3F4, whose epitope does not contain any tyrosine residues (Figure 5B).

Acetylation Reaction. Tryptic digestion of rSHaPrP(90−231) theoretically generates a maximum of 17 peptides; however, tryptic cleavage at K−P and R−P peptide bonds is incomplete and variable, a circumstance that affects cleavage of K_{101}-P_{102}, K_{104}-P_{105}, R_{136}-P_{137}, and R_{164}-P_{165} peptide bonds (Table 1 of the Supporting Information). In rSHaPrP(90−231) samples, we routinely detected G_{90}-K_{106} (the result of missed cleavages at K_{101} and K_{104}), H_{111}-R_{136}, P_{137}-R_{148}, Y_{149}-R_{151}, E_{152}-R_{156}, Y_{157}-R_{164}, P_{165}-K_{185}, Q_{186}-K_{194}, G_{195}-K_{204}, V_{209}-K_{220}, and E_{221}-R_{229}. We also detected additional peptides resulting from missed cleavages, like Y_{157}-K_{185}, Q_{186}-K_{204}, and E_{221}-R_{230}

(Figure 2 and Table 2 of the Supporting Information). The small peptides T_{107}-K_{110} and I_{205}-R_{208} and the single-amino acid "peptides" R_{230} and S_{231} were not detected. Similar results were obtained with SHaPrP 27−30 samples treated with PNGase F; in untreated samples, signals from peptides P_{165}-K_{185} and G_{195}-K_{204}, which are variably glycosylated, were too small to be clearly discerned from baseline noise or altogether missing. Analysis of Ac$_2$O-treated samples is complicated by the fact that upon acetylation, lysine residues are rendered resistant to tryptic cleavage. This means that reaction products are found on runoff peptides reaching to the next lysine or arginine residue, but often such peptides are too long to be efficiently extracted after in-gel digestion or ionize poorly during MALDI. Digestion with chymotrypsin or gluC, each of which hydrolyzes peptide bonds at residues other than lysine and therefore should prevent these problems, was attempted. However, the distribution of target residues within the PrP sequence resulted in an abundance of either overly long or overly short peptides that provided very little additional information (data not shown). As a consequence, analysis focused mainly on the amino-terminal peptide G_{90}-K_{106}, which escaped these limitations because it contains two internal lysine residues (K_{101} and K_{104}) and the amino terminus (G_{90}). This peptide provided extremely useful information about solvent exposure of this important region in rSHaPrP(90−231) and SHaPrP 27−30. Ac$_2$O modified very extensively this peptide in both rSHaPrP(90−231) and SHaPrP 27−30 (Figure 6 and Table 1). Acetylation of lysine or terminal amino groups results in a mass increase of 42 Da. Peaks corresponding to mass increases of 42, 84, and 126 Da indicate that both K_{101} and K_{104}, besides the amino terminus (which is more reactive than ε-amino groups of lysine residues, as a consequence of its lower pK_a value, and therefore is certain to be acetylated), react with Ac$_2$O. On the other hand, acetylation of K_{106} would prevent its cleavage by trypsin and therefore cannot be directly assessed. No traces of acetylated G_{90}-K_{110} were detected, although the absence of a peak cannot be interpreted as definitive proof of the absence of that peptide in the sample. However, the presence of intense peaks corresponding to mono-, di-, and triacetylated G_{90}-K_{106}, all dependent on cleavage at K_{106}, strongly suggests that this residue does not suffer extensive acetylation. Of note, virtually no unacetylated G_{90}-K_{106} remained detectable in either rSHaPrP(90−231) or SHaPrP 27−30. A roughly similar distribution of ratios of the intensity of peaks corresponding to mono-, di-, and triacetylated peptides suggests a roughly similar extent of solvent exposure of the amino terminus in rSHaPrP-(90−231) and SHaPrP 27−30.

Relative acetylation of other lysine residues could be assessed only in a very qualitative and approximate way. Modest
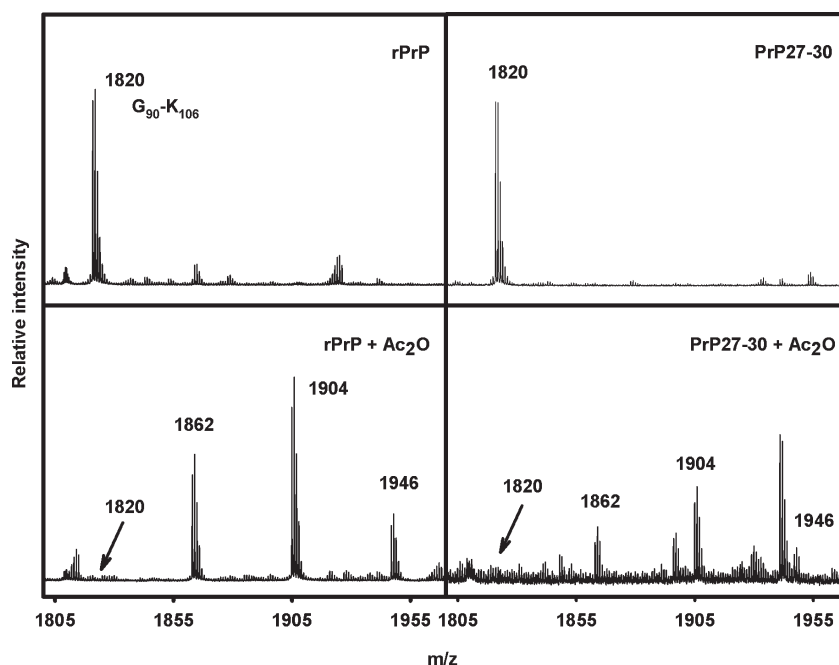
Figure 6. Close-up of the m/z 1820 region of the spectrum shown in Figure 2, corresponding to control and Ac_2O-treated samples. Peaks with m/z values of +42, +84, and +126 reflect mono-, di-, and triacetylation.

acetylation of K_{220} in both rSHaPrP(90−231) and SHaPrP 27−30, reaching similar levels, is surmised by detection of a peptide with masses of 2625.19 Da, corresponding to V_{209}-(AcK_{220})-R_{229}, and 2781.24 Da, corresponding to V_{209}-(AcK_{220})-R_{230}, together with a concomitant decrease in the intensity of peaks corresponding to V_{209}−K_{220}, E_{221}−R_{229}, and E_{221}−R_{230}. Acetylation of the majority of lysine residues in the region spanning K_{110}−K_{194} can be surmised from overall decreases in the intensity of all tryptic peptides corresponding to this region upon acetylation, together with the detection of acetylated, internally uncleaved longer peptides (Table 2 of the Supporting Information). Overall, a moderately higher level of modification seems to occur in rSHaPrP(90−231) versus that in SHaPrP 27−30.

■ DISCUSSION

Understanding the structure of PrP^{Sc} continues to be one of the major challenges in prion research. Without minimal knowledge of the structure of PrP^{Sc}, understanding the mechanism of prion propagation, the basis for the existence of strains, and species barriers, will be impossible, and substantial advances in the rational design of anti-prion drugs will be unlikely. Unfortunately, the insoluble nature of PrP^{Sc} has made efforts to determine its structure extraordinarily difficult, as high-resolution techniques such as NMR or X-ray crystallography cannot be applied. In this context, a number of experimental approaches have provided low-resolution structural information and constraints about PrP^{Sc},[13−28] which have inspired a number of theoretical models. At times, the same experimental data have been interpreted with completely different models.[18,20,37,38]

In our study, we have used chemical surface labeling to gain some structural insight into PrP^{Sc}. We have treated rSHaPrP-(90−231) and SHaPrP 27−30 isolated from scrapie-infected hamster brains with chemical reagents that specifically react with

tyrosine (TNM) and lysine residues (Ac_2O). Via comparison of differences in the reactivity of specific locations within the common sequence of both isoforms of PrP, it is possible to identify regions that undergo conformational changes during conversion of PrP^C to PrP^{Sc}. Reactivity of a given tyrosine or lysine residue toward TNM or Ac_2O is governed by a number of factors, including steric hindrance, hydrogen bonding, and the presence of neighboring charged residues; however, the overall dominant factor is solvent exposure.[29] Nevertheless, a number of previous studies have shown that a direct proportionality between reactivity and solvent exposure cannot always be derived; instead, comparative data can be best used to identify domains and regions that engage in conformational change.[29] In this context, several clear conclusions can be derived from our study. On one hand, tyrosine nitration experiments clearly show a conformational change in the C-terminus of PrP^{Sc}. Both Y_{225} and Y_{226}, very solvent exposed in PrP^C and, accordingly, very reactive toward TNM, are much less so in PrP^{Sc}. Because our mass spectrometry-based analyses compare GPI-containing SHaPrP 27−30 with rSHaPrP(90−231), which does not have a GPI anchor, such decreased reactivity might be a consequence of steric hindrance of the GPI affecting Y_{225} and Y_{226} in the former but not in the latter PrP samples. However, our immunoassay using antibody R1 rules out this possibility, as it showed more decreased reactivity of R1 after TNM treatment in the control (containing $SHaPrP^C$) as compared to the scrapie sample (containing mostly $SHaPrP^{Sc}$). Because $SHaPrP^C$ contains GPI, the difference cannot be ascribed to any GPI-related effect. This agrees with the fact that the GPI moiety, while located in the vicinity, is five amino acid residues from Y_{226} and, further, is flexible,[39] which would limit steric hindrance effects. The diminished solvent exposure of Y_{225} and Y_{226} must therefore be interpreted as a consequence of a structural rearrangement of the C-terminus. Such structural change might affect the secondary, tertiary, and quaternary structure of the PrP molecule. Some

theoretical models of PrP^{Sc20,37,38} propose the permanence of the two C-terminal α-helices of PrP^C, H2 and H3, in PrP^{Sc}. These two α-helices might be packed to form a pile in the PrP^{Sc} assembly, with little change in their tertiary structure.[20] Packing of H3 might result in some structural constraints on residues Y_{225} and Y_{226}; however, it seems very unlikely that these alone would be sufficient to impose significant steric hindrance on a small reagent such as TNM. On the other hand, more significant changes in tertiary structure might take place if the two helices need to change their positions relative to one another. For example, they might be packed in a very tight fashion so that they both rest in the same plane; i.e., the whole α-helical assembly is completely flat, with an elevation of just one α-helix per PrP^{Sc} monomer.[40] This would require torsions and displacements of the two helices resulting in a loss of solvent exposure of Y_{225} and Y_{226}.

The notion that the C-terminal helices might be preserved in PrP^{Sc} derives from immunochemical studies[25] and considerations of the relative percentages of secondary structure based on FTIR analyses.[13−15] Immunochemical studies show that antibody R1, whose epitope comprises C-terminal amino acid residues 225−231, binds to both PrP^C and PrP^{Sc}, although binding to PrP^{Sc} is less intense;[25] R1 is also able to immunoprecipitate both PrP isoforms. These results seem to suggest that the C-terminal epitope is equally accessible to R1 in both PrP isoforms; however, they were performed using PrP^{Sc} that had been dispersed into liposomes, which causes extensive disaggregation of fibrils.[41] Therefore, they can be reconciled with a decreased reactivity of Y_{225} and Y_{226} toward TNM as a consequence of tight packing leading to changes in quaternary and perhaps tertiary structure in the PrP^{Sc} aggregate.

FTIR analyses of full-length PrP^{Sc} and PrP 27−30 indicate the presence of a substantial fraction of α-helical secondary structure, which suggests the permanence of α-helices H2 and H3.[13−15] However, these results should be taken very cautiously, as the assignments of different absorption peaks to specific types of secondary structure have been made on the basis of data obtained with soluble, globular proteins, which might result in significant misassignments when the same protocols are applied to highly packed amyloid proteins such as PrP^{Sc}. As an example, FTIR typically overestimates the percentage of β-sheet in some proteins exhibiting β-helical architectures whose structure has been unambiguously determined by X-ray crystallography, as a consequence of misassignment of absorption bands that actually correspond to tightly packed loops or side chain interactions.[3,42]

Alternatively, conversion of PrP^C to PrP^{Sc} might involve a profound rearrangement of the two C-terminal α-helices, with changes in their secondary structure. Recent studies of recombinant PrP amyloid fibers generated by PMCA using PrP^{Sc} seeds suggest that the C-terminus of these PrP polymers displays β-sheet secondary structure. In particular, hydrogen−deuterium exchange analyses show that the region from approximately residue 163 to the C-terminus displays very slow exchange rates, typical of β-strands;[43] of note, the region of residues 225−231 displays an intermediate protection that suggests it might be just at the border of an extended β-sheet-rich core, but it is more protected than the same region in monomeric PrP.[43,44] These fibers are infectious, although their relative infectivity is several orders of magnitude lower than that of PrP^{Sc} isolated from infected brains, and whether the structures of these recombinant PrP^{Sc}-seeded fibers and PrP^{Sc} are similar remains to be seen. Evidence of a massive disruption of the C-terminal pair of α-helices

in recombinant PrP amyloid fibers has been presented by the Surewicz group using site-directed spin labeling, which also suggests tight packing of PrP monomers within the amyloid assembly.[45,46]

A second conclusion from our experiments is that the region spanning $Y_{149}−R_{164}$ undergoes a conformational change, during the transition from PrP^C to PrP^{Sc}, resulting in an increased level of solvent exposure. This suggests an important structural rearrangement of the short β-sheet and α-helix H1 of PrP^C. Our results agree with those of Paramithiotis et al., who found increased exposure of a YYR epitope, either (149)YYR(151) or, more likely, (162)YYR(164), in PrP^{Sc}, as compared to PrP^C. Such an epitope is recognized by a PrP^{Sc}-specific antibody but is cryptic in PrP^C, suggesting a rearrangement of β-strand 2 and/or α-helix 1 during the conversion of PrP^C to PrP^{Sc}.[47] Paramithiotis et al. conclude that the epitope "unmasked" in PrP^{Sc} is likely to be (162)YYR(164), based on the fact that recognition by their specific antibody is not hampered by previous binding of antibody 6H4, whose epitope partially overlaps with (149)YYR(151), although their data do not exclude a partial contribution of this epitope to the overall immunoreactivity. Our mass spectrometry-based data confirm that both epitopes become exposed in PrP^{Sc}. On the other hand, Govaerts et al[20]. have suggested that these regions change to an extended loop in PrP^{Sc}, which would be consistent with altered solvent accessibility. However, limited proteolysis studies suggest that the stretch spanning from approximately G_{142} to R_{151} has a relatively high resistance to PK and therefore might correspond to a β-strand.[23] Given that Y_{149} and Y_{150} are contiguous, if they were part of a β-strand one of them would necessarily face inward, which would be compatible with the fact that only one of these residues, Y_{149}, is increasingly accessible to nitration in SHaPrP 27−30.

The pattern of nitration of rPrP tyrosine residues in this study agrees remarkably well with data from Lennon et al.[29] The overall higher reactivity of TNM in our study might be explained by the higher pH of our reaction buffer (7.5 as opposed to 5.5 in theirs), which would result in a higher concentration of intermediate reactive tyrosinates.[29,48] The only important difference between both studies is the lack of nitration of Y_{218} in ours. Of note, this residue displays an intermediate degree of solvent exposure.

Strikingly, patterns of tyrosine residue nitration in SHaPrP 27−30 and in the recombinant β-oligomer reported in both studies are also very similar, in particular, with regard to the decreased reactivity of Y_{225} and Y_{226} and increased reactivity of tyrosine residues in the $Y_{149}−R_{164}$ region. This means that the same regions of PrP^C undergo conformational changes to convert to PrP^{Sc} or to the recombinant β-oligomer, and that the resulting local structures of these two molecules might share structural similarities. Elucidating the exact nature and extent of these similarities will require additional studies. However, recent fiber X-ray diffraction analyses suggest that the general architecture of PrP^{Sc} and that of recombinant PrP amyloid fibers are different. In particular, PrP^{Sc} does not produce the equatorial ~10.5 Å reflection typical of flat, paired β-sheets, whereas recombinant PrP amyloid fibers do.[28]

Our acetylation data clearly show that the amino terminus of SHaPrP 27−30 is extremely available and solvent-exposed. This result agrees with our previous study in which G_{90} was a major target of chemical modification with the amino group-specific bifunctional reagent bis(sulfosuccinimidyl) suberate (BS^3).[24] However, it does not agree with the trimeric model proposed by Govaerts et al.,[20] which places amino termini in the interior of

the trimeric assembly, unavailable to reaction. We found that solvent accessibility extends to position K_{104}, but most likely not to K_{106}.

In summary, our data identify several regions of PrP^C that undergo structural changes during its conversion to PrP^{Sc} and provide information about the overall solvent exposure and/or availability of different regions of PrP^{Sc}. They confirm that the amino terminus of PrP 27—30, up to position K_{106}, is very solvent-exposed; the region around Y_{128}, located at the end of the "hydrophobic core", becomes less available. Conversely, the region between Y_{149} and R_{164} and in particular Y_{162} and/or Y_{163} become increasingly exposed, suggesting important changes affecting the short β-sheet and α-helix H1; finally, the carboxy terminus becomes less exposed in PrP 27—30 as compared to PrP^C, suggesting important structural changes that might affect the quaternary, tertiary, and/or secondary structure of this region.

These data do not agree with some key features of proposed theoretical models of PrP^{Sc20} and in general should help validate and construct structural models of PrP^{Sc}.

■ ASSOCIATED CONTENT

ⓢ Supporting Information. Theoretical tryptic digestion of SHaPrP(90—231) (Table 1), MALDI-TOF analysis of Lys-containing rSHaPrP(90—231) and SHaPrP 27—30 peptides produced by trypsin digestion after Ac$_2$O modification (Table 2), and MS/MS spectrum of mononitrated (149)YYR(151). This material is available free of charge via the Internet at http://pubs.acs.org.

■ AUTHOR INFORMATION

Corresponding Author
*Department of Microbiology, School of Medicine, University of Santiago de Compostela, Rua de S. Francisco s/n 15782, Santiago de Compostela, Spain. Phone and fax: +34-981-559904. E-mail: jesus.requena@usc.es.

■ ACKNOWLEDGMENT

■ ABBREVIATIONS

Ac$_2$O, acetic anhydride; α-CHC, (R)-cyano-4-hydroxycinnamic acid; BS^3, bis(sulfosuccinimidyl) suberate; BSE, bovine spongiform encephalopathy; CD, circular dichroism; MALDI-TOF, matrix-assisted laser desorption ionization time-of-flight; PK, proteinase K; PMCA, protein misfolding cyclic amplification; PNGase F, N-glycosidase F; PrP, prion protein; PrP^C, cellular isoform of the prion protein; PrP^{Sc}, scrapie isoform of the prion protein; PrP 27—30, proteinase K-resistant core of PrP^{Sc}; rPrP, recombinant prion protein; rSHaPrP(90—231), recombinant Syrian hamster PrP(90—231); SDS—PAGE, sodium dodecyl sulfate—polyacrylamide gel electrophoresis.; TFA, trifluoroacetic acid; TNM, tetranitromethane.

■ REFERENCES

(1) Prusiner, S. B. (1998) Prions. *Proc. Natl. Acad. Sci. U.S.A.* 95 13363–13383.

(2) Aguzzi, A., and Polymenidou, M. (2004) Mammalian prion biology: One century of evolving concepts. *Cell* 116, 1–20.

(3) Requena, J. R. (2009) Structure of mammalian prions. *Future Virol.* 4, 295–307.

(4) Ross, E. D., Minton, A., and Wickner, R. B. (2005) Prion domains: Sequences, structures and interactions. *Nat. Cell Biol.* 7, 1039–1044.

(5) Si, K., Lindquist, S., and Kandel, E. R. (2003) A neuronal isoform of the aplysia CPEB has prion-like properties. *Cell* 115, 879–891.

(6) Ironside, J. W. (1998) Prion diseases in man. *J. Pathol.* 186 227–234.

(7) Wadsworth, J. D., and Collinge, J. (2007) Update on human prion disease. *Biochim. Biophys. Acta* 1772, 598–609.

(8) Harman, J. L., and Silva, C. J. (2009) Bovine spongiform encephalopathy. *J. Am. Vet. Med. Assoc.* 234, 59–72.

(9) Jarrett, J. T., and Lansbury, P. T., Jr. (1993) Seeding "one-dimensional crystallization" of amyloid: A pathogenic mechanism in Alzheimeŕs disease and scrapie? *Cell* 73, 1055–1058.

(10) Bartz, J. C., Bessen, R. A., McKenzie, D., Marsh, R. F., and Aiken, J. M. (2000) Adaptation and selection of prion protein strain conformations following interspecies transmission of transmissible mink encephalopathies. *J. Virol.* 74, 5542–5547.

(11) Bessen, R. A., and Marsh, R. F. (1994) Distinct PrP properties suggest the molecular basis of strain variation in transmissible mink encephalopathy. *J. Virol.* 68, 7859–7868.

(12) Safar, J., Wille, H., Itri, V., Groth, D., Serban, H., Torchia, M., Cohen, F. E., and Prusiner, S. B. (1998) Eight prion strains have PrP(Sc) molecules with different conformations. *Nat. Med.* 10, 1157–1165.

(13) Pan, K. M., Baldwin, M., Nguyen, J., Gasset, M., Serban, A., Groth, D., Mehlhorn, I., Huang, Z., Fletterick, R. J., Cohen, F. E., and Prusiner, S. B. (1993) Conversion of α-helices into β-sheets features in the formation of the scrapie prion proteins. *Proc. Natl. Acad. Sci. U.S.A.* 90, 10962–10966.

(14) Caughey, B., Dong, A., Bhat, K. S., Ernst, D., Hayes, S. F., and Caughey, W. S. (1991) Secondary structure analysis of the scrapie-associated protein PrP 27—30 in water by infrared spectroscopy. *Biochemistry* 30, 7672–7680.

(15) Caughey, B., Raymond, G. J., and Bessen, R. A. (1998) Strain-dependent differences in β-sheet conformations of abnormal prion protein. *J. Biol. Chem.* 273, 32230–32235.

(16) McKinley, M. P., Meyer, R. K., Kenaga, L., Rahbar, F., Cotter, R., Serban, A., and Prusiner, S. B. (1991) Scrapie prion rod formation in vitro requires both detergent extraction and limited proteolysis. *J. Virol.* 65, 1340–1351.

(17) Sim, V. L., and Caughey, B. (2009) Ultrastructures and strain comparison of under-glycosylated scrapie prion fibrils. *Neurobiol. Aging* 12, 2031–2042.

(18) Wille, H., Michelitsch, M., Guénebaut, V., Supattapone, S., Serban, A., Cohen, F. E., Agard, D. A., and Prusiner, S. B. (2002) Structural studies of the scrapie prion protein by electron crystallography. *Proc. Natl. Acad. Sci. U.S.A.* 99, 3563–3568.

(19) Wille, H., Govaerts, C., Borovinskiy, A., Latawiec, D., Downing, K. H., Cohen, F. E., and Prusiner, S. B. (2007) Electron crystallography of the scrapie prion protein complexed with heavy metals. *Arch. Biochem. Biophys.* 467, 239–248.

(20) Govaerts, C., Wille, H., Prusiner, S. B., and Cohen, F. E. (2004) Evidence for assembly of prions with left-handed β-helices into trimers. *Proc. Natl. Acad. Sci. U.S.A.* 101, 8342–8347.

(21) Zou, W. Q., Capellari, S., Parchi, P., Sy, M. S., Gambetti, P., and Chen, S. G. (2003) Identification of novel proteinase K-resistant

C-terminal fragments of PrP in Creutzfeldt-Jakob disease. *J. Biol. Chem.* 278, 40429–40436.

(22) Zanusso, G., Farinazzo, A., Prelli, F., Fiorini, M., Gelati, M., Ferrari, S., Righetti, P. G., Rizzuto, N., Frangione, B., and Monaco, S. (2004) Identification of distinct N-terminal truncated forms of prion protein in different Creutzfeldt-Jakob disease subtypes. *J. Biol. Chem.* 279, 38936–38942.

(23) Sajnani, G., Pastrana, M. A., Dynin, I., Onisko, B., and Requena, J. R. (2008) Scrapie prion protein structural constraints obtained by limited proteolysis and mass spectrometry. *J. Mol. Biol.* 382, 88–98.

(24) Onisko, B., Fernandez, E. G., Freire, M. L., Schwarz, A., Baier, M., Camiña, F., García, J. R., Rodríguez-Segade Villamarín, S., and Requena, J. R. (2005) Probing PrPSc structure using chemical cross-linking and mass spectrometry: Evidence of the proximity of Gly90 amino termini in the PrP 27—30 aggregate. *Biochemistry* 44 10100–10109.

(25) Peretz, D., Williamson, R. A., Matsunaga, Y., Serban, H., Pinilla, C., Bastidas, R. B., Rozenshteyn, R., James, T. L., Houghten, R. A., Cohen, F. E., Prusiner, S. B., and Burton, D. R. (1997) A conformational transition at the N terminus of the prion protein features in formation of the scrapie isoform. *J. Mol. Biol.* 273, 614–622.

(26) Williamson, R. A., Peretz, D., Pinilla, C., Ball, H., Bastidas, R. B., Rozenshteyn, R., Houghten, R. A., Prusiner, S. B., and Burton, D. R. (1998) Mapping the prion protein using recombinant antibodies. *J. Virol.* 72, 9413–9418.

(27) Nguyen, J. T., Inouye, H., Baldwin, M. A., Fletterick, R. J., Cohen, F. E., Prusiner, S. B., and Kirschner, D. A. (1995) X-ray diffraction of scrapie prion rods and PrP peptides. *J. Mol. Biol.* 252, 412–422.

(28) Wille, H., Bian, W., McDonald, M., Kendall, A., Colby, D. W., Bloch, L., Ollesch, J., Borovinsky, A. L., Cohen, F. E., Prusiner, S. B., and Stubbs, G. (2009) Natural and synthetic prion structure from X-ray fiber diffraction. *Proc. Natl. Acad. Sci. U.S.A.* 106, 16990–16995.

(29) Lennon, C. W., Cox, H. D., Hennelly, S. P., Chelmo, S. J., and McGuirl, M. A. (2007) Probing structural differences in prion protein isoforms by tyrosine nitration. *Biochemistry* 46, 4850–4860.

(30) Zhang, H., Stockel, J., Mehlhorn, I., Groth, D., Baldwin, M. A., Prusiner, S. B., James, T. L., and Cohen, F. E. (1997) Physical studies of conformational plasticity in a recombinant prion protein. *Biochemistry* 36, 3543–3553.

(31) Requena, J. R., Dimitrova, M. N., Legname, G., Teijeira, S., Prusiner, S. B., and Levine, R. L. (2004) Oxidation of methionine residues in the prion protein by hydrogen peroxide. *Arch. Biochem. Biophys.* 432, 188–195.

(32) Diringer, H., Beekes, M., Ozel, M., Simon, D., Queck, I., Cardone, F., Pocchiari, M., and Ironside, J. W. (1997) Highly infectious purified preparations of disease-specific amyloid of transmissible spongiform encephalopathies are not devoid of nucleic acids of viral size. *Intervirology* 40, 238–246.

(33) Raymond, G. J., and Chabry, J. (2004) Purification of the pathological isoform of the prion protein (PrP^Sc or PrP^res) from transmissible spongiform encephalopathy-affected brain tissue. In *Techniques in Prion Research* (Lehman, S., and Grassi, J., Eds.) pp 16—26, Birkhauser, Basel, Switzerland.

(34) Laemmli, U. K. (1970) Cleavage of structural proteins during the assembly of the head of bacteriophage T4. *Nature* 227, 680–685.

(35) Shevchenko, A., Wilm, M., Vorm, O., and Mann, M. (1996) Mass spectrometric sequencing of proteins silver-stained polyacrylamide gels. *Anal. Chem.* 68, 850–858.

(36) Carven, G. J., and Stern, L. (2005) Probing the ligand-induced conformational change in HLA-DR1 by selective chemical modification and mass spectrometric mapping. *Biochemistry* 44, 13625–13637.

(37) DeMarco, M., and Daggett, V. (2004) From conversion to aggregation: Protofibril formation of the prion protein. *Proc. Natl. Acad. Sci. U.S.A.* 101, 2293–2298.

(38) DeMarco, M. L., Silveira, J., Caughey, B., and Daggett, V. (2006) Structural properties of prion protein protofibrils and fibrils: An experimental assessment of atomic models. *Biochemistry* 45 15573–15582.

(39) Rudd, P. M., Wormald, M. R., Wing, D. R., Prusiner, S. B., and Dwek, R. A. (2001) Prion glycoprotein: Structure, dynamics, and roles for the sugars. *Biochemistry* 40, 3759–3766.

(40) Langedijk, J. P. M., Fuentes, G., Boshuizen, R., and Bonvin, A. M. J. J. (2006) Two-rung model of a left-handed β-helix for prions explains species barrier and strain variation in transmissible spongiform encephalopathies. *J. Mol. Biol.* 360, 907–920.

(41) Gabizon, R., McKinley, M. P., Groth, D., Kenaga, L., and Prusiner, S. B. (1988) Properties of scrapie prion protein liposomes. *J. Biol. Chem.* 263, 4950–4955.

(42) Khurana, R., and Fink, A. L. (2000) Do parallel β-helix proteins have a unique Fourier transform infrared spectrum? *Biophys. J.* 78 994–1000.

(43) Smirnovas, V., Kim, J. I., Lu, X., Atarashi, R., Caughey, B., and Surewicz, W. K. (2009) Distinct structures of scrapie prion protein (PrP^Sc)-seeded versus spontaneous recombinant prion protein fibrils revealed by hydrogen/deuterium exchange. *J. Biol. Chem.* 284 24233–24241.

(44) Lu, X., Wintrode, P. L., and Surewicz, W. K. (2007) β-Sheet core of human prion protein amyloid fibrils as determined by hydrogen/deuterium exchange. *Proc. Natl. Acad. Sci. U.S.A.* 104, 1510–1515.

(45) Cobb, N. J., Sönnichsen, F. D., Mchaourab, H., and Surewicz, W. K. (2007) Molecular architecture of human prion protein amyloid: A parallel, in-register β-structure. *Proc. Natl. Acad. Sci. U.S.A.* 104 18946–18951.

(46) Cobb, N. J., Apetri, A. C., and Surewicz, W. K. (2008) Prion protein amyloid formation under native-like conditions involves refolding of the C-terminal α-helical domain. *J. Biol. Chem.* 283, 34704–34711.

(47) Paramithiotis, E., Pinard, M., Lawton, T., LaBoissiere, S., Leathers, V. L., Zou, W. Q., Estey, L. A., Lamontagne, J., Lehto, M. T., Kondejewski, L. H., Francoeur, G. P., Papadopoulos, M., Haghighat, A., Spatz, S. J., Head, M., Will, R., Ironside, J., O'Rourke, K., Tonelli, Q., Ledebur, H. C., Chakrabartty, A., and Cashman, N. R. (2003) A prion protein epitope selective for the pathologically misfolded conformation. *Nat. Med.* 9, 893–899.

(48) Bruice, T. C., Gregory, M. J., and Walters, S. L. (1968) Reactions of tetranitromethane. I. Kinetics and mechanisms of nitration of phenols by tetranitromethane. *J. Am. Chem. Soc.* 90, 1612.